iScience

CellPress
OPEN ACCESS

Article

Dynamic lateralization in contralateral-projecting corticospinal neurons during motor learning

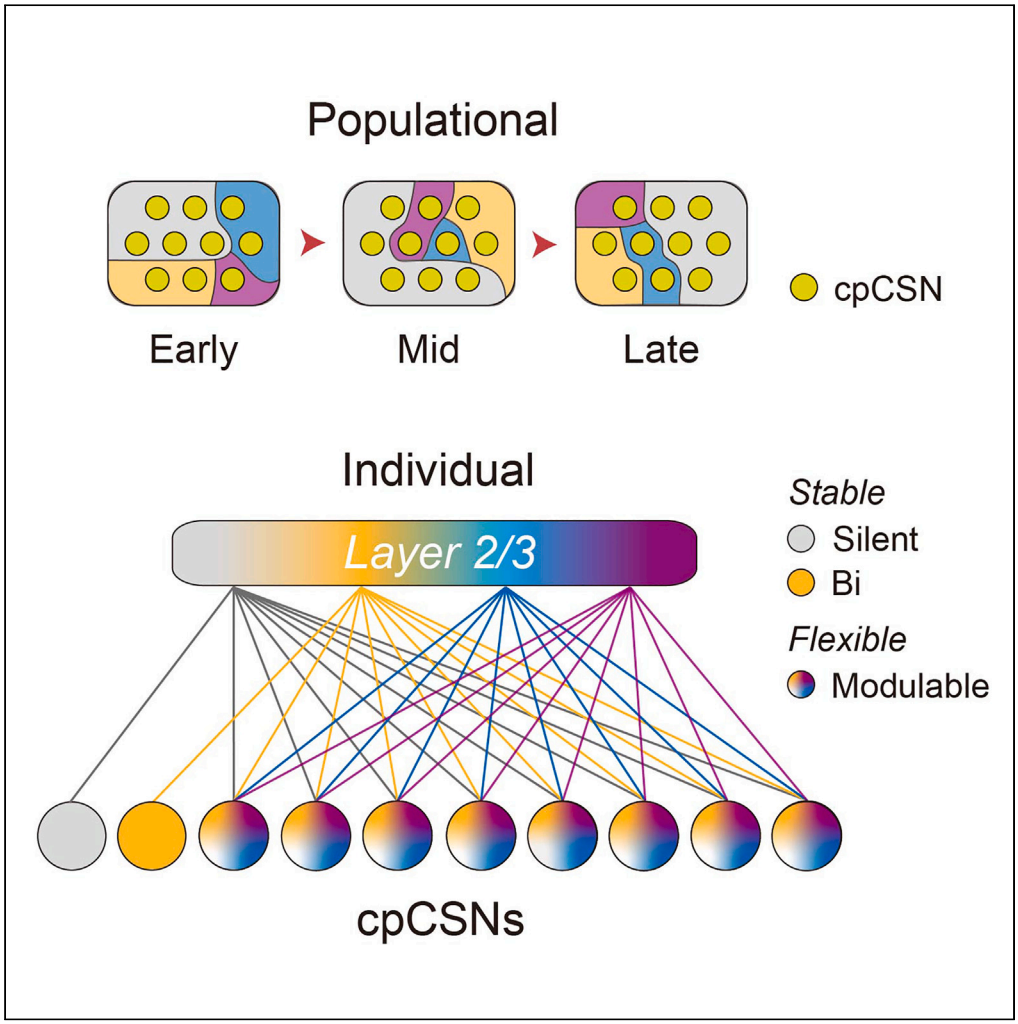

Jiawei Han, Ruixue Wang, Minmin Wang, ..., Shaomin Zhang, Wang Xi, Hemmings Wu

shaomin@zju.edu.cn (S.Z.)
xw333@zju.edu.cn (W.X.)
hemmings@zju.edu.cn (H.W.)

Highlights

cpCSNs exhibit dynamic lateralization during bilateral motor learning tasks

Individual cpCSNs dynamically shift preferences between ipsilateral and contralateral tasks

Laterality-dependent plasticity in cpCSNs offers insights into neuromotor rehabilitation

Han et al., iScience 27, 111078
November 15, 2024
https://doi.org/10.1016/j.isci.2024.111078

iScience

CellPress
OPEN ACCESS

Article

Dynamic lateralization in contralateral-projecting corticospinal neurons during motor learning

Jiawei Han,[1,2,9] Ruixue Wang,[3,4,9] Minmin Wang,[4] Zhihua Yu,[5] Liang Zhu,[6,7] Jianmin Zhang,[1,2] Junming Zhu,[1,2] Shaomin Zhang,[4,*] Wang Xi,[7,8,*] and Hemmings Wu[1,2,10,*]

SUMMARY

Understanding the adaptability of the motor cortex in response to bilateral motor tasks is crucial for advancing our knowledge of neural plasticity and motor learning. Here we aim to investigate the dynamic lateralization of contralateral-projecting corticospinal neurons (cpCSNs) during such tasks. Utilizing *in vivo* two-photon calcium imaging, we observe cpCSNs in mice performing a "left-right" lever-press task. Our findings reveal heterogeneous populational dynamics in cpCSNs: a marked decrease in activity during ipsilateral motor learning, in contrast to maintained activity during contralateral motor learning. Notably, individual cpCSNs show dynamic shifts in engagement with ipsilateral and contralateral movements, displaying an evolving pattern of activation over successive days. It suggests that cpCSNs exhibit adaptive changes in activation patterns in response to ipsilateral and contralateral movements, highlighting a flexible reorganization during motor learning This reconfiguration underscores the dynamic nature of cortical lateralization in motor learning and offers insights for neuromotor rehabilitation.

INTRODUCTION

The motor cortex (MC) is considered to play an important role in motor skill learning.[1] Motor skill learning is compromised when the integrity of MC is impaired.[2–6] Plasticity at multiple levels of the MC is implicated during motor learning, including changes in dendritic spines and neuronal activity in different layers, inputs from subcortical structures, and stimulation threshold and cortical mapping to evoke movement.[7–13]

Two types of learning-related plasticity are reported in the MC. On the one hand, the activity of the MC neurons is closely correlated with movement during learning.[14,15] On the other hand, the relationship between the MC neuronal activity and movement is highly dynamic.[10,15–17] Furthermore, it has been shown that the role of the motor cortex in the execution of well-learned motor skills may become less critical.[2,18] This duality in plasticity represents a balance between stable neural patterns, which underpin the precise execution of well-learned motor skills, and dynamic neural adaptations, which allow for the learning of new movements and adjustment of existing ones, illustrating the MC's pivotal role in both the acquisition and refinement of motor skills. This balance ensures the motor system's adaptability and efficiency, facilitating both the consolidation of motor memory and the flexibility required for continuous learning. Such a duality has also been reported in the plasticity of the corticospinal neuron (CSN), the main output of the MC in layer 5 during motor learning.[8,14,16,17,19,20] It has been suggested that the activity of CSN is highly consistent with movement in the limbs. This conjecture has been confirmed in recent studies that the consistency between CSN activity and movement is better than that of layer 2/3 neurons in the MC. However, CSN also shows dynamic plasticity during motor learning, and the relationship between an individual CSN and movement fluctuates with learning.[9,17] Approximately 90% of the CSNs terminate in the contralateral spinal cord to form a single synaptic connection,[17,21] while sending axon branches to the ipsilateral subcortical structures, pons, and bilateral spinal cord at upper levels.[21,22] These contralateral-projecting CSNs (cpCSNs) are the

[1]Department of Neurosurgery, Second Affiliated Hospital, School of Medicine, Zhejiang University, Hangzhou 310058, China
[2]Clinical Research Center for Neurological Disease of Zhejiang Province, Hangzhou 310058, China
[3]Department of Neurosurgery, Third Affiliated Hospital, Naval Medical University, Shanghai 200438, China
[4]Qiushi Academy for Advanced Studies, Key Laboratory of Biomedical Engineering of Ministry of Education, Zhejiang Provincial Key Laboratory of Cardio-Cerebral Vascular Detection Technology and Medicinal Effectiveness Appraisal, Zhejiang University, Hangzhou 310027, China
[5]Department of Critical Care Medicine, Hangzhou Third People's Hospital, Hangzhou 310058, China
[6]Interdisciplinary Institute of Neuroscience and Technology (ZIINT), College of Biomedical Engineering and Instrument Science, Zhejiang University, Hangzhou 310027, China
[7]Interdisciplinary Institute of Neuroscience and Technology (ZIINT), the Second Affiliated Hospital, School of Medicine, Zhejiang University, Hangzhou 310020, China
[8]MOE Frontier Science Center for Brain Research and Brain Machine Integration, Key Laboratory of Biomedical Engineering of Ministry of Education, College of Biomedical Engineering and Instrument Science, Zhejiang University, Hangzhou 310027, China
[9]These authors contributed equally
[10]Lead contact
*Correspondence: shaomin@zju.edu.cn (S.Z.), xw333@zju.edu.cn (W.X.), hemmings@zju.edu.cn (H.W.)
https://doi.org/10.1016/j.isci.2024.111078

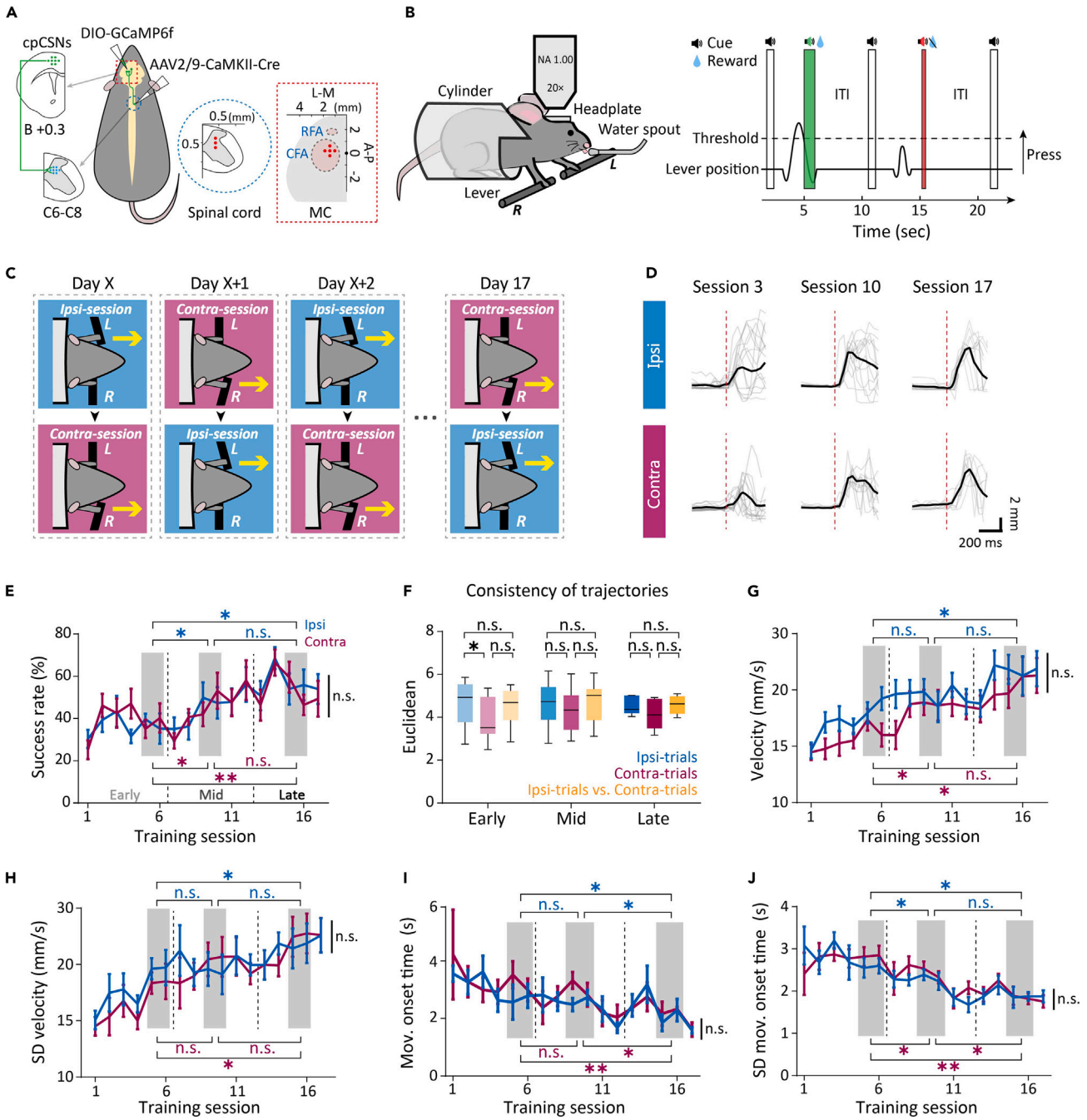

Figure 1. Virus injection and the "left-right" lever-press task

(A) Schematic of injections to selectively express GCaMP6f in corticospinal neurons (cpCSNs). Blue circle represents the viral injection region in the right cervical spinal cord (C6-C8), and red square represents the viral injection region in the left caudal forelimb area (CFA), posterior to the rostral forelimb area (RFA). Red dots represent the viral injection sites. Green line represents GCaMP6f-expressing cpCSNs projecting from layer V in CFA to the cervical spinal cord in C6-C8.

(B) Behavioral setup of the ipsilateral and contralateral lever-press task. Left: the mouse was trained to push the left (or right) lever with the corresponding forepaw for a water reward. Right: passing the lever position threshold after a start cue (black horn and white bar) resulted in a water reward (blue droplet) and a success cue (green horn and bar), or in white noise (red horn and bar) without a reward. ITI: inter-trial interval.

(C) The task consisted of ipsilateral or contralateral sessions each day, alternating daily.

(D) Lever trajectories of sessions 3, 10, and 17 in an example mouse. Top: ipsilateral trials. Bottom: contralateral trials. Gray lines: single movements from randomly selected 15 rewarded trials; black lines: average of these trials; red dashed line: movement onset.

Figure 1. *Continued*

(E) Success rate comparison between ipsilateral and contralateral trials showed no significant difference ($p > 0.05$, two-way repeated-measures ANOVA, $n = 10$ mice from sessions 1 to 17, mean ± SEM). Success rates improved over the course of learning (comparison with average values at early (sessions 5, 6), mid (sessions 9, 10), and late (sessions 15, 16) learning stages; $n = 10$ mice; $^*p < 0.05$, $^{**}p < 0.01$, n.s., not significant, Mann-Whitney U test).

(F) Euclidean distances within ipsilateral trials, contralateral trials, and between trial types at different learning stages (significant difference noted at the early stage between ipsilateral and contralateral trials, $p < 0.05$; n.s., not significant, two-sample t-test, mean ± SEM).

(G–J) Analyses of mean velocity, variability in velocity, movement onset time, and variability in movement onset time revealed improvements over learning sessions, and no significant differences between ipsilateral and contralateral trials (n.s., not significant, $^*p < 0.05$, $^{**}p < 0.01$, p values from two-way repeated-measures ANOVA and Mann-Whitney U tests as appropriate, mean ± SEM).

major output of regular spiking neurons in layer 5, and regular spiking neurons encode bilateral movement information. Whether and how cpCSNs modulate bilateral movement remains unclear.

Here we aim to investigate the dynamics of cpCSN representation of bilateral movement during motor learning. First, we investigate whether cpCSNs carry ipsilateral movement information, and second, if such is the case, how motor information on ipsilateral and contralateral movements is distributed among cpCSNs.

RESULTS

Two-photon calcium imaging of contralateral-projecting corticospinal neurons during a "left-right" motor task

To investigate the dynamics of contralateral-projecting CSNs (cpCSNs) in ipsilateral and contralateral movement during learning, we used the Cre-FLEX system to selectively image cpCSNs under a two-photon microscope. This was achieved by a combination of adeno-associated virus encoding the calcium indicator GCaMP6f (AAV2/9-EF1α-DIO-GCaMP6f) injection in the left caudal forelimb area (CFA) and AAV encoding Cre recombinase (AAV2/9-CaMKII-Cre) injection into the C6 to C8 segments of the right spinal cord (Figure 1A; STAR Methods). Fluorescence of cpCSNs was observed 2 weeks after injection, however, the long-term imaging of somas in layer 5 was not possible due to their depth. Instead, we imaged apical dendritic trunks in layer 2/3 (Figures S1 and S2; Table S1), as their calcium events showed a high correlation with those of the somas, serving as a reliable proxy.[17,23] To stably record the activity of dendritic trunks, we used vessels in the field of view (FOV) for image alignment (Figure S1). Due to technical limitations, we were not able to acquire stable recordings in every session; classified neurons in each stage with stable recordings were averaged across sessions.

Over a period of 3 weeks, mice ($n = 9$) were trained daily in both an ipsilateral session and a contralateral session on a left-right lever-press task, with task difficulty gradually increasing in the first 5 days (Figures 1B and S3). This task was adapted from traditional lever-press and Right-Left Pedal tasks.[24,25] The "left-right" lever-press task consisted of two parts to dissociate the movement of ipsilateral and contralateral limbs so that neuron activity could be recorded respectively. In the ipsilateral session, water-restricted mice learned to use their left (ipsilateral) forelimb to press the left lever for a water reward, and conversely, used their right (contralateral) forelimb in the contralateral session. The duration of each session was 10 min, and the order of ipsilateral and contralateral sessions was reversed every day (Figures 1C and S3). Lever trajectories on both sides became more consistent with training over time (Figure 1D). The lever press performance—measured by success rates, consistencies, velocities, and response times—improved significantly during motor learning in both ipsilateral and contralateral movement and showed no significant difference between the two sides (Figures 1E–1J). These results suggested that mice were able to learn the "left-right" lever-press task at a similar level.

Neural representation of contralateral-projecting corticospinal neurons during bilateral movements

We then investigated the neuronal activity of cpCSNs during ipsilateral and contralateral movements. Similar to previous findings in motor cortical neurons, some cpCSNs were active during movements, while others remained inactive (Figures 2A and 2B).[9,17,18,25,26] We categorized cpCSNs into task-related (active) neurons and silent neurons based on their calcium events during movements (STAR Methods). Additionally, active cpCSNs exhibited heterogeneity during bilateral movements. Neurons active solely during ipsilateral movements were classified as ipsilateral-preferring (ipsi-preferring) neurons. In contrast, neurons active only during contralateral movements were classified as contralateral-preferring (contra-preferring) neurons. Neurons active and inactive during both ipsilateral and contralateral movements were classified as bilateral-preferring (bi-preferring) neurons and silent neurons, respectively (Figures 2B–2D and S4; STAR Methods). These findings suggested that cpCSNs were involved in the control of both ipsilateral and contralateral movements.

The dynamics of laterality in contralateral-projecting corticospinal neuron ensembles during motor learning

To further elucidate the dynamics of cpCSNs during motor learning, we quantified the proportions of ipsi-, contra-, bi-preferring, and silent neurons at different stages of learning (Table S2). We found no significant changes in the proportions of silent neurons (early: 60.03 ± 4.51%, mid: 54.72 ± 5.7%, late: 47.05 ± 4.63%; mean ± SEM), and bi-preferring neurons (early: 16.78 ± 3.37%, mid: 21.4 ± 4.96%, late: 22.5 ± 5.33%; mean ± SEM; Figure 3A) across stages. However, the proportion of ipsi-preferring neurons was significantly higher in the early and late compared to the middle stage (early: 16.31 ± 1.53%, mid: 8.81 ± 1.23%, late: 17.83 ± 2.79%; mean ± SEM; Figure 3A), while the proportion of contra-preferring neurons was significantly lower in the early stage relative to the middle and late stages (early: 6.88 ± 1.03%, mid: 15.04 ± 2.33%, late: 12.57 ± 2.06%; mean ± SEM; Figure 3A). Overall, active cpCSNs showed an increasing trend in activity during contralateral motor learning, and a decreasing trend in activity during ipsilateral motor learning (Figure S5). These

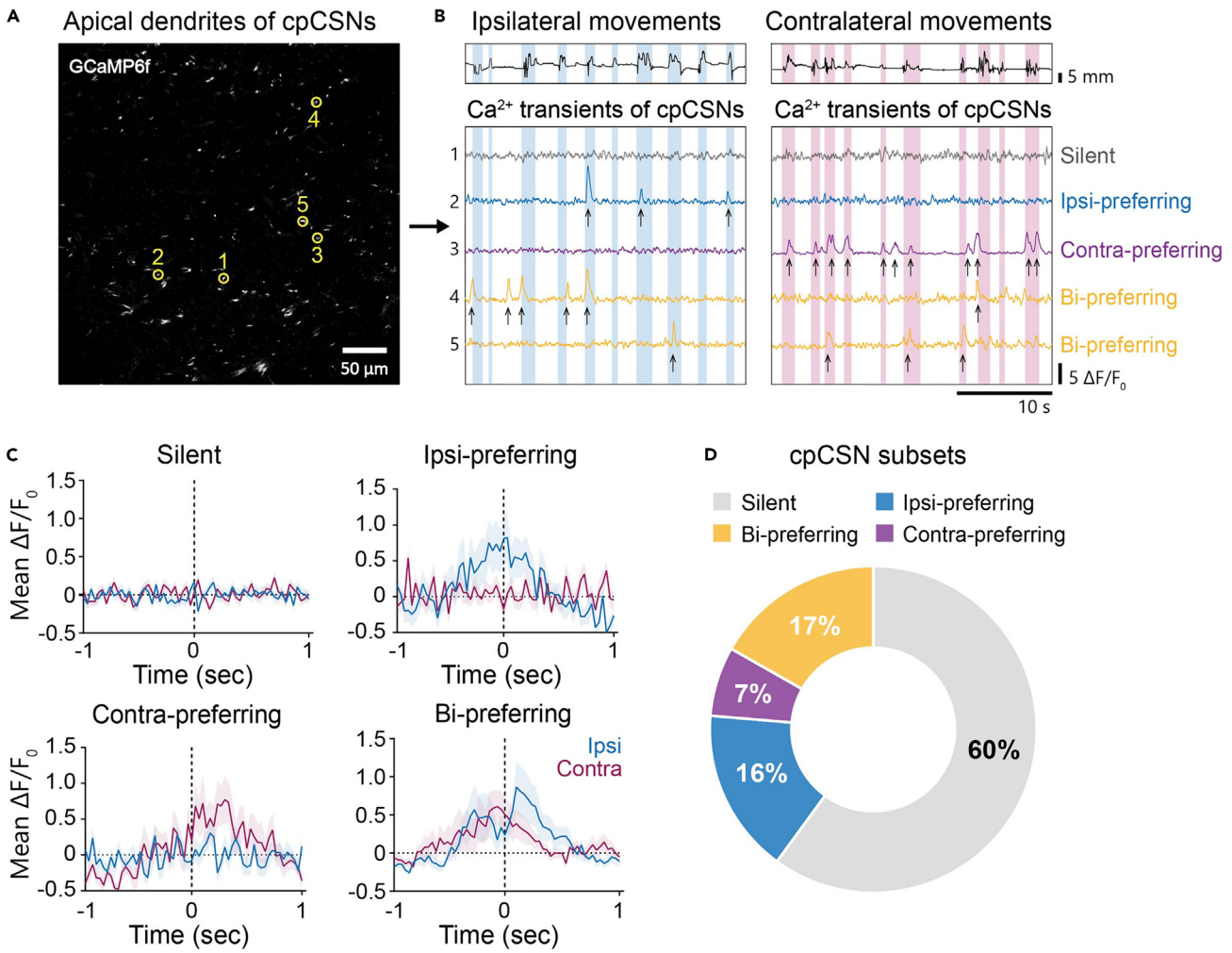

Figure 2. Heterogeneity of cpCSNs in ipsilateral and contralateral movements

(A) Two-photon (2p) image showing GCaMP6f expression in apical dendrites of contralateral-projecting corticospinal neurons (cpCSNs) with example regions of interest (ROIs) highlighted in yellow.

(B) Activity of the example ROIs from (A) during movements in a representative mouse. Top: lever position for ipsilateral and contralateral movements, with green highlighted regions indicating detected movements. Bottom: calcium transients of silent, ipsi-preferring, contra-preferring, and bi-preferring cpCSNs, with arrows marking detected calcium events.

(C) Mean $\Delta F/F_0$ of example cpCSNs subsets across 30 randomly selected ipsilateral (ipsi) trials and 30 contralateral (contra) trials (mean ± SEM).

(D) Proportional distribution of early-stage cpCSN subsets.

alterations in the proportions of ipsi- and contra-preferring neurons suggested laterality-related plasticity within cpCSN ensembles during bilateral motor learning.

The cumulative distribution of the laterality index among the cpCSN ensemble revealed an ipsilateral preference at the early stage, a contralateral preference at the middle stage, and no discernible preference at the late stage (Figure 3B). The mean laterality index at the level of individual mice followed a similar pattern (laterality index: early: −0.57 ± 0.1, mid: 0.24 ± 0.19, late: −0.04 ± 0.15; mean ± SEM; Figure 3C). To determine whether these changes in ensemble laterality were attributable to shifts in ipsi- and contra-preferring neurons or bi-preferring neurons, we analyzed the mean laterality index of bi-preferring neurons at different stages. No significant changes were found between stages (laterality index: early: 0.002 ± 0.005, mid: 0.006 ± 0.005, late: 0.013 ± 0.009; mean ± SEM; Figures 3D and S6), indicating that the dynamics of ipsi- and contra-preferring neurons were the primary contributors to the laterality dynamics in cpCSNs.

Laterality-dependent plasticity of contralateral-projecting corticospinal neurons during motor learning

Based on these findings, it appeared to us that the changes in the percentages of ipsilateral- and contralateral-preferring cpCSNs were complementary to each other (i.e., there was an increase in contralateral-preferring and a decrease in ipsilateral-preferring neurons from the early

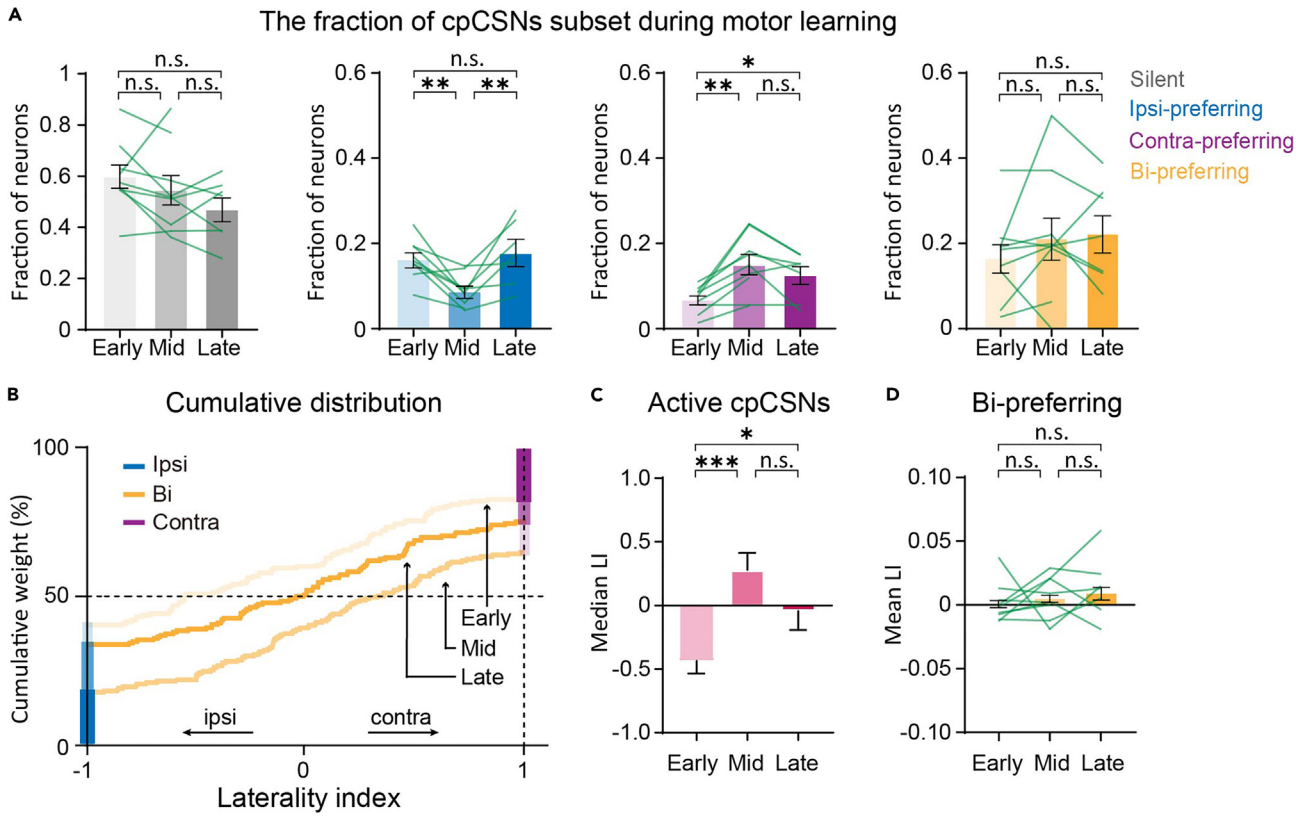

Figure 3. Dynamics of cpCSN Laterality During Motor Learning

(A) Proportions of classified cpCSNs at different learning stages are shown: early and middle stages (n = 9 mice, 548 neurons in total) and late stage (n = 7 mice, 385 neurons in total). Statistical significance was determined using a paired sample t-test (n.s., not significant; *p < 0.05; **p < 0.01). Data are presented as mean ± SEM.

(B) Cumulative distribution of the laterality indices (LI) for all active cpCSNs at the early (high transparency), middle (medium transparency), and late (opacity) stages of learning. LI value of −1 (blue lines) represents ipsi-preferring neurons, and LI value of 1 (purple lines) represents contra-preferring neurons. All other active neurons with LI values between −1 and 1 (yellow lines) represent bi-preferring neurons.

(C) Median LI of all movement-related cpCSNs across different stages (n = 385 neurons from 7 mice, n.s., not significant, *p < 0.05, **p < 0.01, independent-sample t-test, mean ± SEM).

(D) Mean LI of bi-preferring neurons at different stages (n.s., not significant, paired sample t-test, mean ± SEM).

to the middle stage, and vice versa from the middle to the late stage, Figure S5). To further confirm this hypothesis, we investigated the activities of individual neurons during ipsilateral and contralateral motor learning tasks. The laterality classifications of individual cpCSNs from the early, middle, and late stages are shown in Figures 4A–4D. We found that only 26.8% of the ipsilateral-preferring neurons in the early stage changed their preference to contralateral in the middle stage (Figure 4E). Similarly, only 16.6% of the contralateral-preferring neurons in the middle stage changed their preference to ipsilateral in the late stage (Figure 4F). These findings indicated that the changes we observed at the population level may not accurately reflect individual neuronal dynamics. At the level of individual neurons, only nine of the 67 bi-preferring cpCSNs (13.4%) and 39 of the 212 silent cpCSNs (18.4%) remained unchanged throughout the motor learning task. The majority of the cpCSNs, including 86.6% of the bi-preferring and 81.6% of the silent cpCSNs, as well as all of the ipsilateral- and contralateral-preferring cpCSNs, changed their laterality preference (Figure 4G). The laterality dynamic index suggested that silent cpCSNs were the most stable group of neurons in terms of laterality preference while ipsilateral-preferring cpCSNs showed a significantly higher dynamic index (Figure 4H). The cpCSNs were categorized based on the number of changes in laterality preference, as summarized in Figure 4I, suggesting that more than 85% of cpCSNs changed preference between every learning session. Given the flexible laterality of individual cpCSNs across sessions, we investigated their stability within a single session by comparing the average intensity of calcium events between the first and second halves of the session. The results indicated that both the population and individual neuronal activities of cpCSNs remained relatively stable within the same session, regardless of the learning stage, suggesting a fixed pattern of activity and laterality within a session (Figure S7). Additionally, we observed a significantly higher correlation between neuronal activity and the movement trajectories of correct trials compared to incorrect trials, indicating learning-related dynamics in cpCSNs. Furthermore, while the correlation between neuronal activity and lever-press trajectories remained stable across sessions, contra-preferring neurons exhibited an overall weaker correlation with movements compared to bi-preferring neurons (Figure S8).

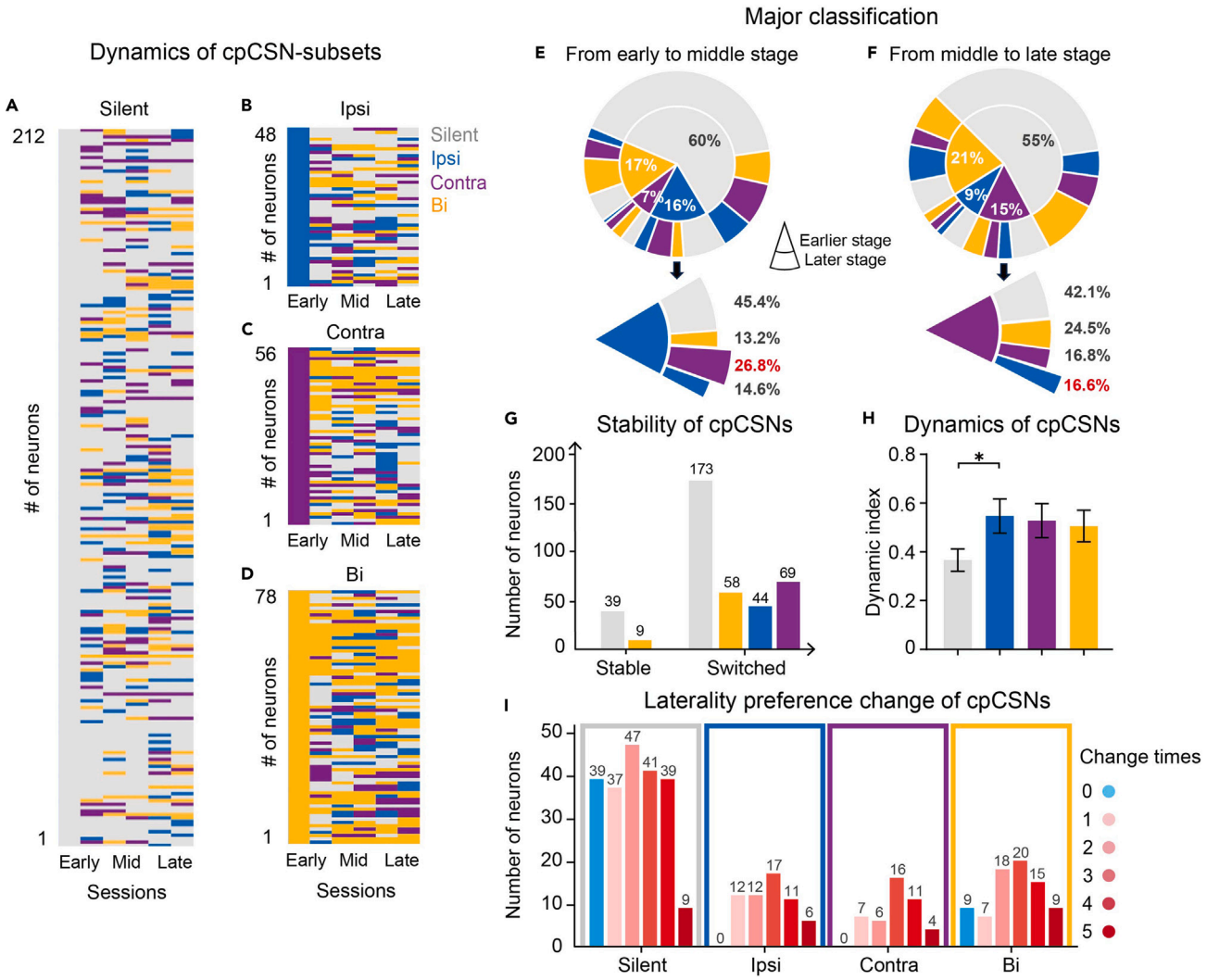

Figure 4. Versatility of laterality-dependent plasticity in cpCSNs during learning

(A–D) Laterality classifications of individual cpCSNs (394 in total) across 6 learning sessions (sessions 5, 6, 9, 10, 15, 16). This includes silent neurons (A, 212 neurons), ipsilateral-preferring neurons (B, 48 neurons), contralateral-preferring neurons (C, 56 neurons), and bi-preferring neurons (D, 78 neurons) in the first session (session 5).

(E and F) Major classification of cpCSNs, representing the classification with the largest number of days at one stage, from early to middle stage, and from middle to late stage.

(G) The number of cpCSNs that maintained or changed their laterality preference classification during learning.

(H) Dynamic index of cpCSN subsets during learning (*$p < 0.05$, independent-sample t-test, mean ± SEM).

(I) The number of cpCSN subsets and the frequency of changes in their laterality preference during learning.

DISCUSSION

Corticospinal neurons in motor learning

Corticospinal neurons, especially contralateral-projecting corticospinal neurons (cpCSNs), play a crucial role in the diverse modulation observed during motor learning, as evidenced by previous studies.[17,20,23,27–29] Through a bilateral lever-press task, we tracked the activities of cpCSNs' apical dendrites in both ipsilateral and contralateral movements throughout motor learning. Our results uncover dynamic shifts in laterality preferences and proportions of cpCSN subsets over the learning trajectory. A majority of individual cpCSNs displayed malleable laterality preferences, suggesting intricate interactions between cpCSN activities and the laterality of movement.

Dynamics in contralateral-projecting corticospinal neuron ensemble

The motor cortex is known for its high level of plasticity, with neurons disengaging from movement control during motor skill learning.[2,18] Lesions in the motor cortex before training prevented rats from learning a skilled motor task, whereas the same lesions had no noticeable

effect on already acquired skills.[2] Similarly, M1 population activity became more consistent from the early to middle stage as task performance improved. However, from the middle to late stage, M1 population activity became variable again despite the consistency in expert behavior.[18] These results indicate a dissociation between M1 and movements during learning and suggest the capacity of subcortical motor circuits to execute learned skills. More importantly, these studies show that activity in M1 changes dynamically during exercise, without following a fixed pattern of neuronal activity becoming more consistent with movement.

The neuronal activity of cpCSNs is selectively active during ipsilateral or contralateral movements (Figure 2), which highlights the heterogeneity in their laterality preferences and aligns with previous studies.[17,18,24,25] Soma et al. used the Right-Left Pedal task, in which head-restrained male rats manipulated a right or left pedal with the corresponding forelimb, allowing independent monitoring of both forelimb movements with high spatiotemporal resolution, and recorded neuronal activity in the M1 and M2 regions using extracellular multineuronal recordings.[25] They found that in the motor cortex, pyramidal tract neurons in one hemisphere exhibit task-related activity with distinct laterality preferences, including ipsilateral-preferring, contralateral-preferring, and bilateral-preferring, in a newly learned motor task.[25] Peter et al. investigated the plasticity of corticospinal neuron activity during motor learning using *in vivo* two-photon calcium imaging in mice learning a lever-press task and concluded that the relationship between corticospinal neuron activity and movement is dynamic, with individual neurons changing their activity patterns across days, leading to a novel and decorrelated association between corticospinal activity and movement.[17] Steinberg et al. investigated the activity of neuronal populations in the primary motor cortex of rhesus monkeys during unimanual and bimanual arm movements. They found that population vectors constructed from the activity of neurons from the primary motor cortex in one hemisphere accurately predicted the direction of movement for both unimanual and bimanual movements.[30] In addition, a neuron's function typically is determined by its anatomical structure. The bilateral motor control capacity in cpCSNs is structured based on axon branches that extend to the ipsilateral subcortical structures, pons, and bilateral spinal cord at upper levels, eventually terminating in the contralateral spinal cord to form a single synaptic connection.[17,21,22] The functional diversity of cpCSNs may be linked to their axonal lateral branches, which are responsive to different neurotransmitters and undergo distinct modulation during learning periods.[31,32] Overall, these studies demonstrated that cpCSNs displayed high dynamics in their relationship with motor control, and have the potential to encode bilateral movement.

We categorized cpCSNs into four subsets based on laterality preferences. The subset proportions shifted during motor learning (Figure 3), consistent with changes in movement-active and movement-related neuron proportions previously reported.[17,18] Intriguingly, the later learning stages saw a surge in ipsi-preferring neurons, diverging from studies reporting a dominance of contra-preferring pyramidal tract neurons.[25,33] This divergence might stem from our study's focus on cpCSNs, rather than previously studied contralateral-projecting corticopontine neurons. Additionally, different recording methods resulting in a larger neuron sample size in our study could contribute to this discrepancy.[25] Serradj et al. found that the corticospinal tract is essential for executing precise motor tasks, with the transection of this tract impairing performance on precision tasks but not on adaptive tasks. Additionally, training on precision tasks increased the correlation of corticospinal neuron activity, suggesting that learning-mediated changes in corticospinal networks are crucial for the execution of dexterous movements.[34] Task-specific neuronal adaptations to varied motor tasks further suggest that cpCSNs serve multifaceted roles during different learning stages.[23,35,36]

Motor cortex laterality preference: A dynamic output

The dynamic nature of cpCSNs' laterality preference throughout the learning stages is a key aspect of our findings. Individual cpCSNs displayed significant flexibility, with transitions between movement-active and quiescence-active states, indicative of a bidirectionally evolving pattern of activity.[17,18] The motor cortex's task-specific patterns surpass the activity differences due to muscle contraction alone,[19,37,38] reflecting neural ensembles' capacity to buffer against input noise.[17,39–41] Additionally, our results show that the activity patterns in cpCSNs are adaptable during both ipsilateral and contralateral movements in the learning process.

Remarkably, the increase in the proportion of ipsi-preferring neurons from the middle to the late stage of learning did not result from a corresponding decrease in contra-preferring neurons. Instead, this increase comprised changes across all four cpCSN subsets. The primary axons of cpCSNs, which terminate in the contralateral spinal cord, suggest a dominant role in controlling movements of contralateral limbs.[42,43] However, cpCSNs also develop axon collaterals that project subcortical structures on the ipsilateral side, particularly the dorsal striatum.[23] It has been shown that spiny projection neurons (SPNs) in the dorsal lateral striatum, which receive input from the motor cortex, exhibit synaptic plasticity to both ipsilateral and contralateral movements during learning.[8] This indicates that cpCSNs, as precursors to SPNs, may exhibit plasticity in response to bilateral movements during learning phases. Furthermore, the motor task's stereotyped pattern leads to motor skill automatization by subcortical structures, rather than the motor cortex itself,[2,18,26] reducing cortical interference during movement execution.[44]

In conclusion, our study highlights the modulability of cpCSNs in response to laterality preference during bilateral motor learning. These findings offer insights into the potential roles of cpCSNs in motor rehabilitation, demonstrating their capacity to adapt dynamically to varying learning stages and tasks. The versatility and adaptability of cpCSN underscore their importance in the neural mechanisms underlying motor learning, and provide a foundation for future research into their role in motor skill acquisition and rehabilitation.

Limitations of the study

One limitation of our study is the absence of a control experiment for the left-right upper-limb motor learning task, where a random water reward would be used instead of a success cue-triggered water reward. However, a previous study implemented similar control experiments, and demonstrated that a dynamic relationship also existed between neuronal activity and movement in animals not engaged in specific motor learning tasks.[17] We hypothesize that such would be the case for laterality dynamics, too, but would require further experiments to confirm.

Moreover, EMG has been used in previous reports for behavioral studies in the upper and lower limbs of mice.[37,45–47] However, EMG monitoring in these studies has been applied to already learned tasks or innate behaviors, and to the best of our knowledge, no studies have reported forelimb-EMG monitoring during motor learning in mice. We actually tried it in our pilot study, but the mice failed to learn the motor task with the EMG setup. Less traumatic EMG will help us better record muscle activity in mice during upper-limb motor learning, and will further help us better underscore motor learning.

Finally, interventional experiments including the optogenetic inhibition of cpCSNs would significantly enhance our understanding of their role in unilateral limb motor control and motor learning. For example, the inhibition of cpCSNs might influence differently in ipsilateral movement and contralateral movement, which could better demonstrate the role of cpCSNs during bilateral motor learning. This approach should be applied in future research to further explore the function of cpCSNs.

RESOURCE AVAILABILITY

Lead contact

Requests for further information and resources should be directed to and will be fulfilled by the lead contact, Hemmings Wu (hemmings@zju.edu.cn).

Materials availability

This study did not generate new unique reagents.

Data and code availability

- All data reported in this article will be shared by the lead contact upon request.
- All original code has been deposited at GitHub and is publicly available as of the date of publication. DOI is listed in the key resources table.
- Any additional information required to reanalyze the data reported in this article is available from the lead contact upon request.

ACKNOWLEDGMENTS

This work was supported by grants from the National Natural Science Foundation of China [82171519, 82270301, and 82071287], and the National Key R&D Program of China (2022ZD0208605).

AUTHOR CONTRIBUTIONS

J. H., J. Z., W. X., J. Z., S. Z., and H. W. conceived the idea and designed the experiments. J. H., R. W., M. W., and L. Z. conducted the experiments. J. H. and R. W. analyzed data. J. H., R. W., J. Z., S. Z., and H. W. wrote the article. J. H., W. X., Z. Y., J. Z., S. Z., and H. W. revised the article. All authors reviewed and approved the final version.

DECLARATION OF INTERESTS

The authors declare no competing interests.

STAR★METHODS

Detailed methods are provided in the online version of this paper and include the following:

SUPPLEMENTAL INFORMATION

Supplemental information can be found online at https://doi.org/10.1016/j.isci.2024.111078.

Received: February 20, 2024
Revised: June 15, 2024
Accepted: September 27, 2024
Published: October 1, 2024

REFERENCES

1. Sanes, J.N., and Donoghue, J.P. (2000). Plasticity and primary motor cortex. Annu. Rev. Neurosci. *23*, 393–415. https://doi.org/10.1146/annurev.neuro.23.1.393.
2. Kawai, R., Markman, T., Poddar, R., Ko, R., Fantana, A.L., Dhawale, A.K., Kampff, A.R., and Ölveczky, B.P. (2015). Motor cortex is required for learning but not for executing a motor skill. Neuron *86*, 800–812. https://doi.org/10.1016/j.neuron.2015.03.024.
3. Whishaw, I.Q., Alaverdashvili, M., and Kolb, B. (2008). The problem of relating plasticity and skilled reaching after motor cortex stroke in the rat. Behav. Brain Res. *192*, 124–136. https://doi.org/10.1016/j.bbr.2007.12.026.
4. Guo, J.-Z., Graves, A.R., Guo, W.W., Zheng, J., Lee, A., Rodríguez-González, J., Li, N., Macklin, J.J., Phillips, J.W., Mensh, B.D., et al. (2015). Cortex commands the performance of skilled movement. Elife *4*, e10774. https://doi.org/10.7554/eLife.10774.
5. Whishaw, I.Q., Pellis, S.M., Gorny, B., Kolb, B., and Tetzlaff, W. (1993). Proximal and distal impairments in rat forelimb use in reaching follow unilateral pyramidal tract lesions. Behav. Brain Res. *56*, 59–76. https://doi.org/10.1016/0166-4328(93)90022-i.
6. Piecharka, D.M., Kleim, J.A., and Whishaw, I.Q. (2005). Limits on recovery in the corticospinal tract of the rat: partial lesions impair skilled reaching and the topographic representation of the forelimb in motor cortex. Brain Res. Bull. *66*, 203–211. https://doi.org/10.1016/j.brainresbull.2005.04.013.
7. Xu, T., Yu, X., Perlik, A.J., Tobin, W.F., Zweig, J.A., Tennant, K., Jones, T., and Zuo, Y. (2009). Rapid formation and selective stabilization of synapses for enduring motor memories. Nature *462*, 915–919. https://doi.org/10.1038/nature08389.
8. Hwang, F.-J., Roth, R.H., Wu, Y.-W., Sun, Y., Kwon, D.K., Liu, Y., and Ding, J.B. (2022). Motor learning selectively strengthens cortical and striatal synapses of motor engram neurons. Neuron *110*, 2790–2801.e5. https://doi.org/10.1016/j.neuron.2022.06.006.
9. Masamizu, Y., Tanaka, Y.R., Tanaka, Y.H., Hira, R., Ohkubo, F., Kitamura, K., Isomura, Y., Okada, T., and Matsuzaki, M. (2014). Two distinct layer-specific dynamics of cortical ensembles during learning of a motor task. Nat. Neurosci. *17*, 987–994. https://doi.org/10.1038/nn.3739.
10. Tanaka, Y.H., Tanaka, Y.R., Kondo, M., Terada, S.I., Kawaguchi, Y., and Matsuzaki, M. (2018). Thalamocortical Axonal Activity in Motor Cortex Exhibits Layer-Specific Dynamics during Motor Learning. Neuron *100*, 244–258.e12. https://doi.org/10.1016/j.neuron.2018.08.016.
11. Krutky, M.A., and Perreault, E.J. (2007). Motor cortical measures of use-dependent plasticity are graded from distal to proximal in the human upper limb. J. Neurophysiol. *98*, 3230–3241. https://doi.org/10.1152/jn.00750.2007.
12. Frost, S.B., Barbay, S., Friel, K.M., Plautz, E.J., and Nudo, R.J. (2003). Reorganization of remote cortical regions after ischemic brain injury: a potential substrate for stroke recovery. J. Neurophysiol. *89*, 3205–3214. https://doi.org/10.1152/jn.01143.2002.
13. Makino, H., Ren, C., Liu, H., Kim, A.N., Kondapaneni, N., Liu, X., Kuzum, D., and Komiyama, T. (2017). Transformation of Cortex-wide Emergent Properties during Motor Learning. Neuron *94*, 880–890.e8. https://doi.org/10.1016/j.neuron.2017.04.015.
14. Isomura, Y., Harukuni, R., Takekawa, T., Aizawa, H., and Fukai, T. (2009). Microcircuitry coordination of cortical motor information in self-initiation of voluntary movements. Nat. Neurosci. *12*, 1586–1593. https://doi.org/10.1038/nn.2431.
15. Hira, R., Ohkubo, F., Ozawa, K., Isomura, Y., Kitamura, K., Kano, M., Kasai, H., and Matsuzaki, M. (2013). Spatiotemporal dynamics of functional clusters of neurons in the mouse motor cortex during a voluntary movement. J. Neurosci. *33*, 1377–1390. https://doi.org/10.1523/jneurosci.2550-12.2013.
16. Costa, R.M., Cohen, D., and Nicolelis, M.A.L. (2004). Differential corticostriatal plasticity during fast and slow motor skill learning in mice. Curr. Biol. *14*, 1124–1134. https://doi.org/10.1016/j.cub.2004.06.053.
17. Peters, A.J., Lee, J., Hedrick, N.G., O'Neil, K., and Komiyama, T. (2017). Reorganization of corticospinal output during motor learning. Nat. Neurosci. *20*, 1133–1141. https://doi.org/10.1038/nn.4596.
18. Hwang, E.J., Dahlen, J.E., Hu, Y.Y., Aguilar, K., Yu, B., Mukundan, M., Mitani, A., and Komiyama, T. (2019). Disengagement of motor cortex from movement control during long-term learning. Sci. Adv. *5*, eaay0001. https://doi.org/10.1126/sciadv.aay0001.
19. Churchland, M.M., Cunningham, J.P., Kaufman, M.T., Foster, J.D., Nuyujukian, P., Ryu, S.I., and Shenoy, K.V. (2012). Neural population dynamics during reaching. Nature *487*, 51–56. https://doi.org/10.1038/nature11129.
20. Lemon, R.N. (2008). Descending pathways in motor control. Annu. Rev. Neurosci. *31*, 195–218. https://doi.org/10.1146/annurev.neuro.31.060407.125547.
21. Reiner, A., Jiao, Y., Del Mar, N., Laverghetta, A.V., and Lei, W.L. (2003). Differential morphology of pyramidal tract-type and intratelencephalically projecting-type corticostriatal neurons and their intrastriatal terminals in rats. J. Comp. Neurol. *457*, 420–440. https://doi.org/10.1002/cne.10541.
22. Shepherd, G.M.G. (2013). Corticostriatal connectivity and its role in disease. Nat. Rev. Neurosci. *14*, 278–291. https://doi.org/10.1038/nrn3469.
23. Nelson, A., Abdelmesih, B., and Costa, R.M. (2021). Corticospinal populations broadcast complex motor signals to coordinated spinal and striatal circuits. Nat. Neurosci. *24*, 1721–1732. https://doi.org/10.1038/s41593-021-00939-w.
24. Peters, A.J., Chen, S.X., and Komiyama, T. (2014). Emergence of reproducible spatiotemporal activity during motor learning. Nature *510*, 263–267. https://doi.org/10.1038/nature13235.
25. Soma, S., Saiki, A., Yoshida, J., Ríos, A., Kawabata, M., Sakai, Y., and Isomura, Y. (2017). Distinct Laterality in Forelimb-Movement Representations of Rat Primary and Secondary Motor Cortical Neurons with Intratelencephalic and Pyramidal Tract Projections. J. Neurosci. *37*, 10904–10916. https://doi.org/10.1523/jneurosci.1188-17.2017.
26. Hwang, E.J., Dahlen, J.E., Mukundan, M., and Komiyama, T. (2021). Disengagement of Motor Cortex during Long-Term Learning Tracks the Performance Level of Learned Movements. J. Neurosci. *41*, 7029–7047. https://doi.org/10.1523/jneurosci.3049-20.2021.
27. Ueno, M., Nakamura, Y., Li, J., Gu, Z., Niehaus, J., Maezawa, M., Crone, S.A., Goulding, M., Baccei, M.L., and Yoshida, Y. (2018). Corticospinal Circuits from the Sensory and Motor Cortices Differentially Regulate Skilled Movements through Distinct Spinal Interneurons. Cell Rep. *23*, 1286–1300.e7. https://doi.org/10.1016/j.celrep.2018.03.137.
28. Wang, X., Liu, Y., Li, X., Zhang, Z., Yang, H., Zhang, Y., Williams, P.R., Alwahab, N.S.A., Kapur, K., Yu, B., et al. (2017). Deconstruction of Corticospinal Circuits for Goal-Directed Motor Skills. Cell *171*, 440–455.e14. https://doi.org/10.1016/j.cell.2017.08.014.
29. Basista, M.J., and Yoshida, Y. (2020). Corticospinal Pathways and Interactions Underpinning Dexterous Forelimb Movement of the Rodent. Neuroscience *450*, 184–191. https://doi.org/10.1016/j.neuroscience.2020.05.050.
30. Steinberg, O., Donchin, O., Gribova, A., Cardosa de Oliveira, S., Bergman, H., and Vaadia, E. (2002). Neuronal populations in primary motor cortex encode bimanual arm movements. Eur. J. Neurosci. *15*, 1371–1380. https://doi.org/10.1046/j.1460-9568.2002.01968.x.
31. Schiemann, J., Puggioni, P., Dacre, J., Pelko, M., Domanski, A., van Rossum, M.C.W., and Duguid, I. (2015). Cellular mechanisms underlying behavioral state-dependent bidirectional modulation of motor cortex output. Cell Rep. *11*, 1319–1330. https://doi.org/10.1016/j.celrep.2015.04.042.
32. Li, Q., Ko, H., Qian, Z.M., Yan, L.Y.C., Chan, D.C.W., Arbuthnott, G., Ke, Y., and Yung, W.H. (2017). Refinement of learned skilled movement representation in motor cortex deep output layer. Nat. Commun. *8*, 15834. https://doi.org/10.1038/ncomms15834.
33. Rios, A., Soma, S., Yoshida, J., Nonomura, S., Kawabata, M., Sakai, Y., and Isomura, Y. (2019). Differential Changes in the Lateralized Activity of Identified Projection Neurons of Motor Cortex in Hemiparkinsonian Rats. eNeuro *6*, ENEURO.0110-19.2019. https://doi.org/10.1523/eneuro.0110-19.2019.
34. Serradj, N., Marino, F., Moreno-López, Y., Bernstein, A., Agger, S., Soliman, M., Sloan, A., and Hollis, E. (2023). Task-specific modulation of corticospinal neuron activity during motor learning in mice. Nat. Commun. *14*, 2708. https://doi.org/10.1038/s41467-023-38418-4.
35. Rodgers, C.C., Nogueira, R., Pil, B.C., Greeman, E.A., Park, J.M., Hong, Y.K., Fusi, S., and Bruno, R.M. (2021). Sensorimotor strategies and neuronal representations for shape discrimination. Neuron *109*, 2308–2325.e10. https://doi.org/10.1016/j.neuron.2021.05.019.
36. Cao, V.Y., Ye, Y., Mastwal, S., Ren, M., Coon, M., Liu, Q., Costa, R.M., and Wang, K.H. (2015). Motor Learning Consolidates Arc-Expressing Neuronal Ensembles in Secondary Motor Cortex. Neuron *86*, 1385–1392. https://doi.org/10.1016/j.neuron.2015.05.022.
37. Miri, A., Warriner, C.L., Seely, J.S., Elsayed, G.F., Cunningham, J.P., Churchland, M.M., and Jessell, T.M. (2017). Behaviorally Selective Engagement of Short-Latency Effector Pathways by Motor Cortex. Neuron

95, 683–696.e11. https://doi.org/10.1016/j.neuron.2017.06.042.

38. Oby, E.R., Ethier, C., and Miller, L.E. (2013). Movement representation in the primary motor cortex and its contribution to generalizable EMG predictions. J. Neurophysiol. *109*, 666–678. https://doi.org/10.1152/jn.00331.2012.
39. Liberti, W.A., 3rd, Markowitz, J.E., Perkins, L.N., Liberti, D.C., Leman, D.P., Guitchounts, G., Velho, T., Kotton, D.N., Lois, C., and Gardner, T.J. (2016). Unstable neurons underlie a stable learned behavior. Nat. Neurosci. *19*, 1665–1671. https://doi.org/10.1038/nn.4405.
40. Ganguly, K., Dimitrov, D.F., Wallis, J.D., and Carmena, J.M. (2011). Reversible large-scale modification of cortical networks during neuroprosthetic control. Nat. Neurosci. *14*, 662–667. https://doi.org/10.1038/nn.2797.
41. Davidson, A.G., Chan, V., O'Dell, R., and Schieber, M.H. (2007). Rapid changes in throughput from single motor cortex neurons to muscle activity. Science *318*, 1934–1937. https://doi.org/10.1126/science.1149774.
42. Tennant, K.A., Adkins, D.L., Donlan, N.A., Asay, A.L., Thomas, N., Kleim, J.A., and Jones, T.A. (2011). The organization of the forelimb representation of the C57BL/6 mouse motor cortex as defined by intracortical microstimulation and cytoarchitecture. Cerebr. Cortex *21*, 865–876. https://doi.org/10.1093/cercor/bhq159.
43. Overduin, S.A., d'Avella, A., Carmena, J.M., and Bizzi, E. (2012). Microstimulation activates a handful of muscle synergies. Neuron *76*, 1071–1077. https://doi.org/10.1016/j.neuron.2012.10.018.
44. Wolff, S.B.E., Ko, R., and Ölveczky, B.P. (2022). Distinct roles for motor cortical and thalamic inputs to striatum during motor skill learning and execution. Sci. Adv. *8*, eabk0231. https://doi.org/10.1126/sciadv.abk0231.
45. Santuz, A., Laflamme, O.D., and Akay, T. (2022). The brain integrates proprioceptive information to ensure robust locomotion. J. Physiol. *600*, 5267–5294. https://doi.org/10.1113/jp283181.
46. Pearson, K.G., Acharya, H., and Fouad, K. (2005). A new electrode configuration for recording electromyographic activity in behaving mice. J. Neurosci. Methods *148*, 36–42. https://doi.org/10.1016/j.jneumeth.2005.04.006.
47. Warriner, C.L., Fageiry, S., Saxena, S., Costa, R.M., and Miri, A. (2022). Motor cortical influence relies on task-specific activity covariation. Cell Rep. *40*, 111427. https://doi.org/10.1016/j.celrep.2022.111427.
48. Pachitariu, M., Stringer, C., Dipoppa, M., Schröder, S., Rossi, L.F., Dalgleish, H., Carandini, M., and Harris, K.D. (2017). Suite2p: beyond 10,000 neurons with standard two-photon microscopy. Preprint at bioRxiv. https://doi.org/10.1101/061507.
49. Mittmann, W., Wallace, D.J., Czubayko, U., Herb, J.T., Schaefer, A.T., Looger, L.L., Denk, W., and Kerr, J.N.D. (2011). Two-photon calcium imaging of evoked activity from L5 somatosensory neurons *in vivo*. Nat. Neurosci. *14*, 1089–1093. https://doi.org/10.1038/nn.2879.
50. Beaulieu-Laroche, L., Toloza, E.H.S., Brown, N.J., and Harnett, M.T. (2019). Widespread and Highly Correlated Somato-dendritic Activity in Cortical Layer 5 Neurons. Neuron *103*, 235–241.e4. https://doi.org/10.1016/j.neuron.2019.05.014.

STAR★METHODS

KEY RESOURCES TABLE

REAGENT or RESOURCE	SOURCE	IDENTIFIER
Experimental models: Organisms/strains		
Mouse: C57BL/6	SLARC Animal	N/A
Recombinant DNA		
AAV2/9- EF1α-DIO-GCaMP6f-WPRE	BrainVTA	Cat#PT-0106
AAV2/9- CaMKIIα-Cre-WPRE	BrainVTA	Cat#PT-0220
Software and algorithms		
ImageJ	NIH	https://imagej.nih.gov/ij/
MATLAB 2020a	Mathworks	https://www.mathworks.com/
Imaris 8.0	Bitplane	https://imaris.oxinst.com/
Suite2p	Pachitariu, M et al.[48]	https://suite2p.readthedocs.io/en/latest/
QT	The Qt Company	https://www.qt.io/
Code	This paper	https://doi.org/10.5281/zenodo.13725619

EXPERIMENTAL MODEL AND STUDY PARTICIPANT DETAILS

Specimens and ethics

All animal studies and experimental procedures were approved by the Animal Care and Use Committee of the animal facility at Zhejiang University and in accordance with the Institutes of Health Guide for the Care and Use of Laboratory Animals (Approval number: ZJU20220011). A total of 10 adult male mice (C57BL/6J, 8 weeks or older) were used in the experiments. Data from 1 mouse was discarded due to poor imaging results; data from 9 mice was included in the final analysis. Mice were grouped and housed with running wheels in a 12:12 hours reverse light-dark cycle, and all experimental activities were conducted during the dark phase to maintain consistency.

Surgeries and virus injections

Surgical procedures were performed under isoflurane anesthesia (4% for induction and 1.5-2% during surgery) and injected with dexamethasone (2 mg/kg), cefuroxime (5 mg/kg) and buprenorphine (0.1 mg/kg) subcutaneously at the beginning of the surgery to prevent infection, inflammation, and pain. Surgeries consisted of two successive steps, the first being a spinal cord injection, and the second being a cortical injection and cranial window implantation, as described by Peter et al.[17]

For the first step, the back was shaved and cleansed with iodine, alcohol, and saline. A midline incision was then made in the skin, reaching deep into the muscle layer. Muscle was removed and fatty tissue was isolated to fully expose the thoracic vertebrae. Because the spinous process of T2 was prominent, the muscles and ligaments attached to the spine of the C5-T2 segment were located and cleared. The T2 spinous process was clamped and fixed, and the soft tissue on the surface of the C6-C8 segments of the spinal cord was removed. AAV2/9-CaMKII-Cre (BrainVTA Technology, China) inside a glass electrode was injected into three sites on the right side of the spinal cord (200 nL at each site) and placed 0.4 mm from the midline, 0.7 mm from the surface and separated by 0.6 mm rostrocaudally. After the injection, the fixed T2 spinous process was released and the muscle, soft tissue, and skin were sutured sequentially. Subsequently, for cortical injections, we prepared the skull surface and opened a cranial window over the left motor cortex, injecting AAV2/9-EF1α-DIO-GCaMP6f (BrainVTA Technology, China) at five sites in a plus (+) shape in the left motor cortex, each injection was 50 nL and placed 0.7 mm from the surface, separated by 0.5 mm, centered at the left caudal forelimb area (0.3 mm anterior and 1.5mm lateral to Bregma). A 5 mm-diameter glass coverslip was placed over the skull window and secured with medical glue and dental cement. A custom-made metal headplate was then glued to the skull surface and fixed with dental cement. Post-operative care ensured animals displayed no motor deficits, with most resuming wheel running within two days.

Behavior

After recovering from surgery, mice were restricted to a maximum of 1-2 mL water per day for 2 weeks before the training. Mice were then trained daily in a lever-press task during two-photon imaging for 1 ipsilateral session and 1 contralateral session, lasting 10 mins per session. During lever-press task, mice rested their body and hindlimbs in a tube and placed their right forelimb on the fixed right lever and their left forelimb on a movable lever in the ipsilateral session, and vice versa in the contralateral session. The lever consisted of a handle glued to a custom angle encoder. Angle data from the angle encoder was continuously monitored using a customized decoder and software (The QT Company). Presses were defined as the lever being pushed beyond 6 mm and maintained for more than 120 ms before returning to the resting

position. The task consisted of a variable intertrial interval, followed by a 5-10 s cue period during which the lever pressed triggered water reward was delivered. Cue periods paired with a 1-second start cue, rewards paired with a 600-ms high-pitched melodious tone, and a failure to press the lever within the cue period paired with a 200-ms white noise, with an extra 2 s of intertrial interval. The cue period was reduced during the first three sessions from 15 s to 10 s and then to 5 s, and the intertrial interval was increased during the first 5 sessions from 2-3 s to 5-7 s and then to 8-10 s to encourage discrete movements. The duration time was increased from 60 ms to 120 ms and the lever-press threshold was increased from 3 mm to 6 mm during the first four sessions. Each session consisted of approximately 80 trials. Sessions were binned into 3 stages in analyses (early: 1-6; middle: 7-12; late: 13 and after). At the early stage of learning, various behavioral parameters were constantly adjusted to enhance learning until the 5th session, after which the behavioral parameters would remain fixed (Figure S2). The average success rate exceeded 50% on session 12, and as a result, training after session 12 was defined as the late stage.

For all mice, if an ipsilateral session was performed first on one day and a contralateral session was performed after a rest of 5-10 mins, the contralateral session was performed first and then the ipsilateral session was performed on the next day, to prevent the corresponding laterality of mice due to task stereotype.

Two-photon imaging

Before imaging, one dose of 50 μL TRITC-dextran solution (ALADDIN, China) was retro-orbitally injected. Two-photon imaging was conducted through a 20× 1.0 NA (Olympus) mounted on a customized two-photon microscope (2P plus, Bruker Corporation) with a tunable femtosecond laser (Ti: Sapphire laser, Chameleon Ultra II, Coherent Inc.), whose power was controlled by Pockels Cell (EO-PC, Thorlabs Corporation). Dual-channel fluorescent signals (green: 500-550 nm filter, red: 570-620 nm filter) were collected in photomultiplier tubes (PMTs). The wavelength of the imaging laser was first kept at 860 nm with low power (10-50 mW, under objective), so that imaging drifts could be manually monitored and corrected via identification of local vasculature (red channel) and apical dendrites (green channel). Then images were acquired at a rate of ~30 Hz, covering 406.36×406.36 μm with 512×512 square pixels, using a 920 nm laser with low power (10-50 mW, under objective) for 10 mins per session to record the activity of apical dendrites (green channel).

For 3D structural imaging, the field of view was the same size at a rate of ~0.5 Hz with 1024×1024 square pixels, in which each frame was repeated two times on average as structural results. Due to technical limitations, we were not able to acquire stable recordings in every session; classified neurons in each stage with stable recordings were averaged across sessions.

METHOD DETAILS

Lever-press movement analysis

The angle data were down-sampled from 200 Hz to 30 Hz to remove baseline noise. The movement onset time for each lever press was determined by finding when the lever moved away from the baseline position before movements. The movement epoch was defined as -1 s to 1 s around the movement onset. The largest lever angle and the time duration for the lever pushed beyond 5 mm were used as the motion features to further filter out the middle 80% of movements within each session. All filtered lever presses were aligned by the movement onset time for subsequent analyses.

We used Euclidean distance (d) to describe the consistency between different lever trajectories:

$$d(x,y) = \sqrt{\sum_{i=1}^{n}(x_i - y_i)^2}$$

Where x_i and y_i are the lever distances from baseline of two trials, and n is the total number of frames in a movement epoch (n = 60). Euclidean distance between each pair of trajectories from different trials within session or across sessions comprising the mean distance of the sessions were calculated.

Two-photon data analysis

The fluorescence data acquired by the two-photon microscope was first processed by Suite2p,[48] including motion correction, region of interest (ROI) generation, and fluorescence extraction. ROIs were then manually corrected by average image and fluorescent traces.

The average image of each session after motion correction was used to align the imaging data over multiple sessions. The average image of the first session in each mouse was picked as a reference, and the others were aligned to it via vasculature landmarks to perform normalized cross-correlation, and to find the coordinates of the peak. The alignment across sessions was based on the offset found by this correlation. In aligned maps, ROIs were evaluated by the proximity of centroids. If the distance between centroids of the candidate ROI was less than 8.5 pixels, the candidate ROI would be considered the same ROI. Only ROIs stably identified on given imaging sessions were included for all of the following analyses.

Fluorescent traces for each ROI were created by averaging enclosed pixels and subtracting background fluorescence. ROIs with similarity greater than 0.8 were treated as siblings originating from the same soma.[49,50] Final traces for each neuron were derived by weighted averaging the signals of all sibling branch traces across sessions.

The relative change in fluorescent traces for each ROI was using the following formula:

$$\Delta F / F_0 = (F - F_0) / F_0$$

The F_0 was estimated as the baseline of fluorescent traces from a $\pm$ 15 s sliding window. Then $\Delta F/F$ traces of each ROI were aligned by movement onset time, and then averaged across trials.

Ca events were calculated by $\Delta F/F_0$ traces for each ROI.[17] Two thresholds were defined to find active portions and baseline, the former was 3× standard deviation and the latter was 1× standard deviation. Active portions were identified by a 1-s LOESS-smoothed trace crossing the active threshold and extended backward to begin when the baseline threshold was last crossed. Periods with negative slopes during active portions were regarded as inactive. The remaining active portions were characterized as Ca events and set to the difference between the maximum and minimum values within each event, with baseline and inactive portions set to zero.

Movement-related classification

For the definition of silent neurons, we referred to the definition used by Peters et al., where a neuron is considered silent if it has fewer than five fluorescence events during the movement frames.[24] In our research, cpCSNs were classified as movement-related (active) neurons or silent neurons each day. The neuron was classified as a movement-unrelated (silent) neuron on one day if the count of calcium events is less than 5 during movement epochs in both ipsilateral and contralateral sessions.

Laterality index

In calculating laterality, we referred to the method used by Soma et al. that quantified the laterality of individual neurons using the firing rates of each neuron during bilateral movements.[25] Considering the potential distortion in converting fluorescence signals to spikes using deconvolution methods, we prioritized directly using the mean calcium events for quantitative characterization. This approach also helps to avoid the impact of the decay of the calcium indicator when using fluorescence or $\Delta F/F$ directly. Therefore, we defined the laterality of individual neurons by the mean calcium events of each neuron during bilateral movements.

To evaluate the laterality of each active neuron, we calculate calcium events per frame averaged over trials during movement, between ipsilateral and contralateral sessions. The laterality index (LI) was computed using the following formula:

$$\textit{Laterality index} = \begin{cases} (c - i)/(c + i), & \textit{if } c > 0 \textit{ and } i > 0 \\ +1, & \textit{if } c > 0 \textit{ and } i = 0 \\ -1, & \textit{if } i > 0 \textit{ and } c = 0 \end{cases}$$

Where c and i are mean calcium events during contralateral and ipsilateral trials (-1 to 1 s relative to the onset of lever-press), respectively. If this index is 1, the neuron was classified as a contra-preferring neuron. If it is -1, the neuron was classified as an ipsi-preferring neuron. Otherwise, it was classified as a bi-preferring neuron.

Dynamic index

To evaluate the dynamic strength in cpCSNs, we investigated their daily classifications. When the classification of cpCSNs shifts, we marked its change as 1, otherwise as 0. The dynamic index is the sum of the number of classification change divided by the number of sessions minus one.

Neuronal stability calculation

Trials in each of the first half (H1) and second half (H2) sessions were extracted to represent the former and latter periods within sessions, respectively. The correlation between calcium activity and lever-press trajectory of each neuron in the two halves within the session was calculated by Pearson's correlation coefficient (CC), and then the difference in the correlation of neuronal activity and movement between H1 and H2 was analyzed by Wilcoxon's rank-sum test. An in-session stable neuron was defined if there was no significant difference between H1 and H2, and vice versa as an unstable neuron.

QUANTIFICATION AND STATISTICAL ANALYSIS

All statistical analyses were performed using IBM SPSS. The comparison of successful trials and successful rates between ipsilateral and contralateral movement were analyzed using two-way repeated-measures ANOVA. The laterality index of neurons, and the average activity of neurons at different stages during motor learning were analyzed using Mann-Whitney tests and Kruskal Wallis test. The laterality index of neurons in different stages and the activity of neurons between ipsilateral and contralateral movement in the same stage were analyzed with paired sample t-tests. All comparisons using t-tests are two-sided. Differences were considered statistically significant when $p < 0.05$. Error bars indicate standard errors of the mean (SEM) unless noted otherwise.